A Laminar Forced Convective Heat Transfer and Fluid Flow in a Finned Cylindrical Annulus

[1]Isaac K. Adegun, [2*]Olalekan A. Olayemi, [3]Temidayo S. Jolayemi and [2]Oladapo T. Ogunbodede
[1]Department of Mechanical Engineering, University of Ilorin, Ilorin, Kwara State
[2]Department of Aeronautics and Astronautics, Kwara State University, Malete, Kwara State
[3]Department of Mechanical Engineering, Institute of Technology, Kwara State Polytechnic, Kwara State
olalekan.olayemi@kwasu.edu.ng

Abstract— The purpose of this paper is to numerically investigate the effects of some geometric parameters and flow variables on heat transfer augmentation in annuli with equi-spaced internal longitudinal fins along the external walls. A fully developed flow and a constant thermal boundary condition of uniform heat flux at the walls of the pipe were assumed. Continuity, momentum and energy transport equations were adopted for the solutions of the problem. A Q-BASIC code was written based on the finite difference scheme generated. Numerical experiments were conducted to ascertain the effects of Reynolds number *Re*, radius ratio, *R.R*, Prandtl number Pr, fin height H, and pipe inclination Ω, on the rate of heat transfer and fluid flow. The results obtained show that for $50 \leq Re \leq 500$, total Nusselt number Nu_T increases with increase in *Re* while for *Re*> 500, there was no significant increase in Nu_T. Nusselt number, average velocity and bulk temperature of the fluid increase with increasing Ω in the range $0° \leq \Omega \leq 75°$ but for the range $75° \leq \Omega \leq 90°$ the effect is negligible. For *R.R*> 0.6, the heat transfer was observed to be almost independent of *R;* therefore for economic purposes, heat exchangers similar to the configuration studied should be run at a low pumping power. A numerical study was done to validate the program by test running it for the finless annuli for similar boundary conditions; the results obtained in the present work show the same trend as that of Kakac and Yucel.

Keywords—Forced convection, Heat transfer, Fluid flow, Internal fins, Annulus.

1 Introduction

The need to develop more efficient thermal systems to enhance heat transfer has aroused interest over the years. Therefore, heat transfer from rough surfaces have been researched into because of its ability to increase the effectiveness of heat transfer (Mir *et al*., 2004). Laminar forced convective fluid flow and heat transfer arises in a range of engineering problems particularly where viscous fluids are either cooled or heated and the heat transfer involved in this process is low, hence the need for heat augmentation. Dirker and Meyer (2002), Dou *et al*., (2005), Haramoto *et al*., (2002) and Jawarneh (2007) submitted that annulus flow passage is being widely used in aero-engines, turbomachinery, in the reduction of drag force, cooling of the rotor and stator of electric motors and generators, petroleum engineering and various chemical industrial devices. When the need to enhance heat transfer between a solid and an adjourning fluid arises, extended surfaces otherwise known as fins are employed (Incropera & Dewitt, 2002).

Fins are essentially used to increase rate of heat transfer where alternative means are impracticable(Das, 2005). For this reason, the current research introduces fins to enhance heat transfer in annular heat exchangers. The problem of fluid flow and heat transfer is of considerable interest in various applications, as such, the flow in an annulus was analyzed by different researchers to predict flow behaviour and heat transfer; these include Chauhan *et al*., (2014) who investigated numerically the effect of narrow gap on the fluid flow and heat transfer through an eccentric annular region, it was concluded that there was temperature shoot up in the region due to flow mal-Eck distribution with heat removal from the wall surfaces. Ebrahim *et al*., (2013) conducted a numerical study of power-law fluid through eccentric annular geometry, it was found that pipe eccentricity contributes to hole cleaning problems.

Khalil *et al*., (2008) studied experimentally and numerically the flow behaviour in a concentric annulus with a moving core. In the study it was concluded that flow separation was obtained in the case of adverse pressure gradient for the velocity profile. Nobari and Mehrabani (2010) numerically investigated fluid flow and heat transfer in eccentric curved annuli and concluded that heat transfer rate can be augmented in eccentric curved annuli at large Dean numbers depending on the eccentricity and curvature ratio. Ishima *et al*., (2008) carried out an experimental study of the wake flow around a circular cylinder. It was concluded that fins make flow complicated and that the angle of inclination of the cylinder affects length of recirculation zone. Wu and Zhou (2015) investigated numerically heat transfer and pressure drop in two types of longitudinally and internally finned tube, results obtained show that the field synergy degree of the longitudinally ridged and internally finned tube is better than that of bare annular tube.

Eckert and Drake (1972) submitted that when fins are advantageous, the heat transfer is increased by spacing them as near each other as practicable. Kang (2008) studied experimentally the effect of inclination angle on pool boiling heat transfer in an inclined annular tube submerged in a pool of saturated water at atmospheric pressure; it was asserted that heat transfer coefficients increased with increase in inclination angle. Adegun (2007) worked on fluid flow and heat transfer in heated concentric elliptic annuli. He concluded that cross flow

*Corresponding Author

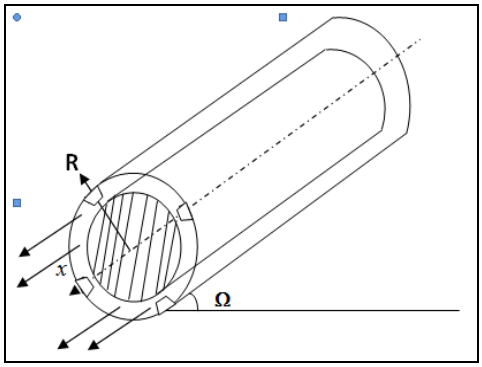

FIG. 1. (a): Cylindrical annulus inclined at an angle Ω to the horizontal

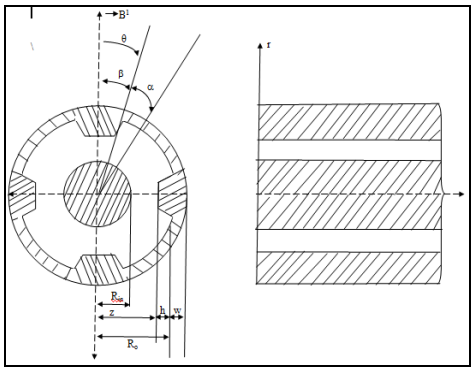

Fig.1(b): Cross section of the finned annulus

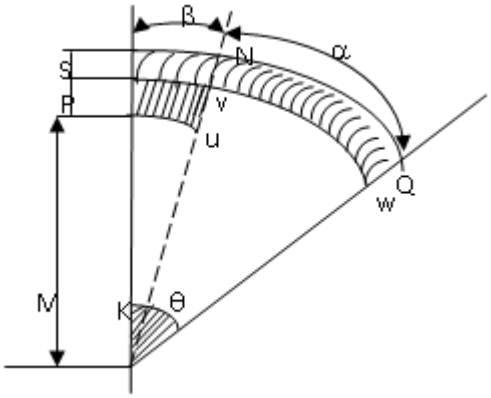

Fig.1(c): Computational Domain

velocities reduces with increasing Reynolds number. Adegun and Bello-Ochende (2004) also studied laminar mixed convective and radiative heat transfer in an inclined rotating rectangular duct with a centered circular tube, this a situation in which fluid flow in the annulus between the outer walls of the inner circular tube and the inner walls of the outer rectangular duct. They obtained a geometric ratio of 0.84 for optimum heat transfer and fluid bulk temperature in the annulus. Rafee (2014) studied the entropy generated in an annuli, the result show that that is a length ratio (L/D_h) at which the entropy generation is maximum.

The present work investigated the effects of variable parameters such as radius ratio, fin height, duct inclination, Prandtl number and Reynolds numbers on heat transfer enhancement for the geometry studied.

2 METHODOLOGY

2.1 Physical Model

The model used for the work was an inclined cylindrical annulus with internal longitudinal fins in the cylindrical coordinate system (r, θ, x) inclined at an angle Ω to the horizontal (Fig.1 (a)). The inclination of the cylinder to the horizontal varied from 0^0 to 90^0 at an interval of 15^0. The geometry of choice for the fins used for the work was made so as to save a reasonable percentage of weight as compared to rectangular fins for equal quantity of heat flow (Eckert & Drake, 1972).The ratio of the duct thermal conductivity to fluid thermal conductivity was embedded into the solution of the governing equations; therefore the fluid flowing in the annulus was generalized.

2.2 Formulation of the Governing Equation

The primitive governing equations are the continuity, momentum and energy transport equations. FollowingDogan and Sivrioglu (2010), these equations can be cast as:

2.2.1 Equation of Continuity

The continuity equation in cylindrical coordinate is gives as,

$$\frac{\partial^2 V_r}{\partial r}+\frac{1}{r}\frac{\partial V_\theta}{\partial \theta}+\frac{\partial V_x}{\partial x}+\frac{V_r}{r}=0 \qquad (1)$$

It is assumed that there is only one non-zero velocity component, namely that in the direction of flow, V_x thus

$$V_r = V_\theta = 0;\ \frac{\partial p}{\partial x}=\frac{\partial p}{\partial \theta} \qquad (2)$$

2.2.2 Momentum Equation

The momentum equation in cylindrical coordinates is expressed as,

$$\frac{\partial^2 V_x}{\partial r^2}+\frac{1}{r}\frac{\partial V_x}{\partial r}+\frac{1}{r^2}\frac{\partial^2 V_x}{\partial \theta^2}=\frac{1}{\mu}\frac{dp}{dx}-\frac{\rho}{\mu}g\sin\Omega \qquad (3)$$

where

$$g_x=-g\sin\Omega \qquad (4)$$

2.2.3 Energy Equation

The energy transport equation is,

$$\frac{\partial^2 T}{\partial r^2}+\frac{1}{r}\frac{\partial T}{\partial r}+\frac{1}{r^2}\frac{\partial^2 T}{\partial \theta^2}=\begin{bmatrix}\frac{V_x}{\alpha}\frac{\partial T}{\partial x} -- fluid\ region\\ 0 -- solid\ \ region\end{bmatrix} \qquad (5)$$

2.3 Transformation Parameters

The following normalization parameters were used to non-dimensionalize equations (1, 2, 3 &5):

$$\Pr = \frac{C_p \mu}{K}\ ; K^* = \frac{k_s}{k_f};$$

$$U = \frac{V_x}{\dfrac{R_0^2\left(\dfrac{-dp}{dx}\right)}{\mu}},$$

$$p_k = \frac{\rho g}{\dfrac{dp}{R_0 d\Gamma}},$$

$$Pe = \frac{2R_0(1-R.R)V_x}{\alpha_t},$$

$$\Gamma = \frac{x}{R_{in} p_e},$$

$$\mathrm{Re}_m = \mathrm{Re}\frac{R_o g}{4(1-R.R)^2 V_x}$$

$$R.R = \frac{R_{in}}{R_0}, R = \frac{r}{R_0},\ W = \frac{w}{R_0}, H = \frac{h}{R_0}\ , \phi = \frac{T - T_0}{\dfrac{q_0 R_0}{K_f}},$$

2.4 Normalized Governing Equations

The non dimensional equations that govern the solution of the problem are:

2.4.1 Normalized Momentum Transport Equation

The non dimensional form of momentum equation is,

$$\frac{\partial^2 U}{\partial R^2} + \frac{1}{R}\frac{\partial U}{\partial R} + \frac{1}{R^2}\frac{\partial^2 U}{\partial \theta^2} = -1 - Pe' \sin\Omega \qquad (6)$$

where

$$Pe' = \frac{\rho g}{\dfrac{dp}{dx}} \qquad (7)$$

2.4.2 Normalized Energy Transport Equation

The non dimensional energy transport equation is,

$$\frac{\partial^2 \phi}{\partial R^2} + \frac{1}{R}\frac{\partial \phi}{\partial R} + \frac{1}{R^2}\frac{\partial^2 \phi}{\partial \theta^2} = \begin{bmatrix} \mathrm{Re}_m U \dfrac{\partial \phi}{\partial \Gamma} - for\ fluid\ region \\ 0 ---- for\ solid\ region \end{bmatrix} \qquad (8)$$

2.5 Applicable Boundary Conditions

By considering Figures (1b) and (1c), the symmetry of the computational domain stipulates the boundary conditions that follow:

a. Region occupied by Fluid (Lines of Symmetry**)**

The two lines of symmetry occur when $\theta = 0$ and $\theta = \alpha + \beta$. For the line of symmetry,

i $$\frac{\partial V_x}{\partial \theta} = 0 \qquad (9)$$

ii

$$\frac{\partial^2 V_x}{\partial \theta^2} = 0 @ \begin{bmatrix} \theta = 0;\ \ R_{in} \le r \le R_o - (R_{in} + h) \\ \theta = \alpha + \beta;\ \ R_{in} \le r \le R_o - R_{in} \end{bmatrix} \qquad (10)$$

b. Interface between Solid and Fluid Regions

For no slip boundary condition, at the walls, the fluid velocity is zero, therefore;

$$V_x = 0\ @ \begin{bmatrix} 0 \le \theta \le \beta;\ \ r = R_o - h \\ \theta = \beta;\ \ R_o - h \le r \le R_o \\ \beta \le \theta \le \alpha + \beta;\ \ r = R_o \\ 0 \le \theta \le \alpha + \beta;\ \ r = R_{in} \end{bmatrix} \qquad (11)$$

Also, the energy equation is subjected to the following boundary conditions:

c. Region occupied by fluid (symmetric condition**)**

$$\frac{\partial T_f}{\partial \theta} = 0 @ \begin{bmatrix} \theta = 0;\ \ R_{in} \le r \le R_o - (R_{in} + h) \\ \theta = \alpha + \beta;\ \ R_{in} \le r \le R_o - R_{in} \end{bmatrix} \qquad (12)$$

d. Solid region (symmetric condition**)**

$$\frac{\partial T_s}{\partial \theta} = 0 @ \begin{bmatrix} \theta = 0;\ \ R_o - h \le r \le R_o + w \\ \theta = \alpha + \beta;\ \ R_o \le r \le R_o + w \end{bmatrix} \qquad (13)$$

e. Outer wall of the tube

$$q_{R_0 + w} = -K_s \left.\frac{\partial T}{\partial r}\right|_{r = R_0 + w} \qquad (14)$$

f. Interface walls between Solid and Fluid

$$T_f = T_s @ \begin{bmatrix} 0 \le \theta \le \beta;\ \ r = R_0 - h \\ \theta = \beta;\ \ R_0 - h \le r \le R_0 \\ \beta \le \theta \le \alpha + \beta;\ \ r = R_0 \\ 0 \le \theta \le \alpha + \beta;\ \ r = R_{in} \end{bmatrix} \qquad (15)$$

2.6 Solution Technique

2.6.1 Finite Difference Analogue of the Normalized Momentum Transport Equation

$$U_{i,j} = \frac{0.5}{\left[\dfrac{1}{(\Delta R)^2} + \dfrac{1}{(R\Delta\theta)^2}\right]} \left\{ \begin{matrix} \left[1 + Pe' Sin\Omega + \left[\dfrac{1}{2R\Delta R} + \dfrac{1}{(\Delta R)^2}\right] U_{i+1,j} + \left[\dfrac{1}{(\Delta R)^2} - \dfrac{1}{2R\Delta R}\right] U_{i-1,j} \right] \\ + \dfrac{1}{(R\Delta\theta)^2}\left[U_{i,j+1} + U_{i,j-1}\right] \end{matrix} \right\} \qquad (16)$$

2.6.2 Finite Difference Analogue of the Normalized Energy Transport Equation

$$\phi_{i,j}^{n}=\frac{0.5}{\left[\frac{U_{i,j}\,\mathrm{Re}_m}{\Delta\Gamma}+\frac{1}{(\Delta R)^2}+\frac{1}{(R\Delta\theta)^2}\right]}\left[\begin{array}{l}2\frac{U_{i,j}\,\mathrm{Re}_m}{\Delta\Gamma}\phi_{i,j}^{n-1}+\left(\frac{1}{(\Delta R)^2}+\frac{1}{(2R\Delta R)}\right)\phi_{i+1,j}^{n}+\\ \left(\frac{1}{(\Delta R)^2}-\frac{1}{(2R\Delta R)}\right)\phi_{i-1,j}^{n}+\left(\frac{2}{(R\Delta\theta)^2}\right)\phi_{i,j+1}^{n}\end{array}\right] \quad (17)$$

where $\phi_{i,j}^{n-1}$ is the temperature at the entrance which is known while $\phi_{i,j}^{n}$, $\phi_{i+1,j}^{n}$, etc. are the unknown temperatures at nodal points in the annulus. By following Welty (1974), an iterative technique was selected for solving this problem. The velocity fields were numerically analyzed by the momentum transport equation and its associated boundary conditions. The energy transport equations were then evaluated for the fluid and solid regions by making use of the velocities obtained from the solution of the momentum equation. The first estimate for the interior values were evaluated by introducing the initial guess values .The iterations were terminated when a prescribed convergence criterion expressed as $\left|Z_i^{(k)}-Z_i^{(k-1)}\right|\le\varepsilon$, Incropera and Dewitt (2002) was satisfied, where Z represents the variable $U\ or\ \phi$, ε represents an error in Z, which is considered to be acceptable for this work when $\varepsilon=10^{-6}$ and k, the iterative counter.

2.7 Evaluation of Nusselt Numbers

The effect of fins in heat transfer augmentation is mainly analyzed by the value of the Nusselt number. The local Nusselt number over the inner cylinder and the outer cylinder are given respectively below by following Padilla (2006):

$$Nu_i=\frac{R_i In\left[\frac{R_o}{R_i}\right]\left.\frac{\partial T}{\partial r}\right|_{r=Ri}}{T_w(x)-T_b(x)} \quad (18)$$

$$Nu_O=\frac{R_0 In\left[\frac{R_o}{R_i}\right]\left.\frac{\partial T}{\partial r}\right|_{r=R_o}}{T_w(x)-T_b(x)} \quad (19)$$

where,

$$T_b(x)=\iint_{Af}T_f v_x r\Delta r R\Delta\theta \Big/ \iint_{Af}v_x r\Delta r\Delta\theta \quad and \quad T_\omega(x)=\int_w Tr\Delta\theta \Big/ \int_w r\Delta\theta$$

3 VALIDATION FOR FLOW IN THE ANNULUS

Fig.2 presents a comparison between the solution obtained in flow in the annulus for the present study and that obtained by Kakaç and Yücel (1974) for flow in an annulus. The present study assumes uniform heat flux in the inner and outer walls of the cylinder while Kakac and Yucel assume a uniform heat flux at the outer wall of the tube and adiabatic condition at the inner wall of the tube. Both plots show that the Nusselt number of the outer wall increases with radius ratio. The slight difference in the imposed boundary conditions in the present work and that of Kakac and Yucel results in the slight variation in the two plots.

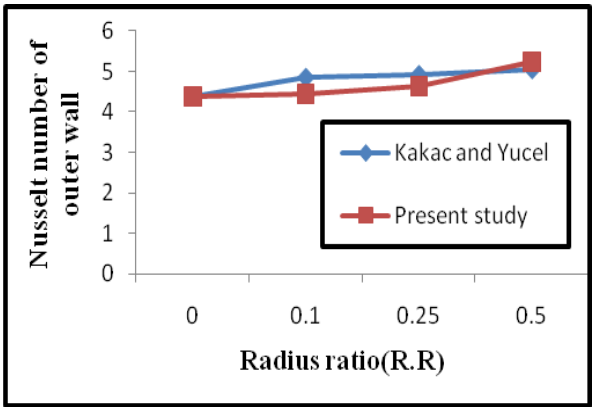

Fig.2. Variation of Outer Nusselt Number with Radius Ratio(R.R)

4 RESULTS AND DISCUSSION

4.1 Overall Heat Transfer Rate

Figure 3 shows the curve that depicts the variation of total Nusselt number with Reynolds number. For $50\le \mathrm{Re}\le 500$ the total Nusselt number increases with increase in Reynolds number. For $\mathrm{Re}>500$, there is no significant increase in total Nusselt number. Therefore, it advisable to run the fluid flow in the configuration at low Reynolds number flow regimes which has an economic advantage of using a low rating pumping machine.

Figure 4 shows the curve for total Nusselt number versus Reynolds number for varying Prandtl numbers For $50\le \mathrm{Re}\le 100$, there is no significant difference in the heat transfer. For $\mathrm{Re}>100$, the total Nusselt number increases with increase in Reynolds number for all Prandtl numbers .This is an indication that that for $\mathrm{Re}<100$, the heat transfer is independent of fluid properties and therefore a function of geometry only.

Figure 5 gives the plots for total Nusselt number versus pipe inclination for various Reynolds numbers. For $0^\circ \le\Omega\le 75^\circ$, the total Nusselt number increases with inclination. For $\Omega>75^\circ$ the total Nusselt number becomes almost invariant indicating that for $75^\circ\le\Omega\le 90^\circ$, the effect of gravity on flow becomes insignificant. This depicts that when applying heat exchangers of this configuration, the inclination should not exceed 75°. This is an indication that the velocity potential of the flow that is required to convect heat is

almost the same in the range of the inclination as revealed by Figure 8 in which the velocity of the flow remains almost a constant value towards the vertical positioning of the duct. Figure 6 is a graph of total Nusselt number versus pipe inclination for various fin heights. The plots show that Nusselt number increases steadily with pipe inclination. Also the figure shows that total Nusselt number increases as fin height increases; this is an indication that the introduction of protrusion into the walls of the tube enhances heat transfer.

Figure 7 is the variation of the total Nusselt number with radius ratio over some Reynolds numbers. The graphs show as the radius ratio increases the heat transfer also increases. This indicates that increase in wetted perimeter augments heat transfer for the geometry under investigation. Furthermore, for R.R> 0.6 the heat transfer is independent of Reynolds number. The pattern of these plots is in agreement with the work of Kakaç and Yücel (1974).

Figure 8 depicts the variation of average velocity of fluid

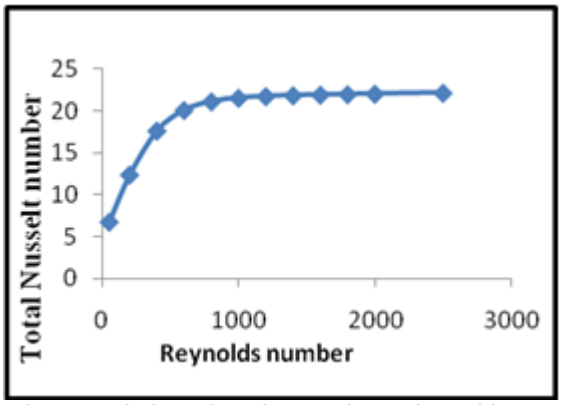

Fig. 3. Variation of total Nusselt number with Reynolds number for: F=4, R.R=0.1, Pr =0.73, W=0.2, β=3°, Ω =0°, H=0.2

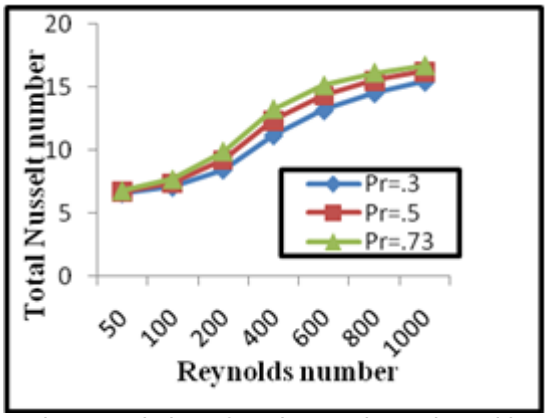

Fig. 4. Variation of total Nusselt number with Reynolds number for F=4, R.R=0.2, W=0.2, H=0.2, =0°, β=3°

with pipe inclination for different radius ratios. The plots depicts that the average velocity of fluid increases significantly with pipe inclination in the

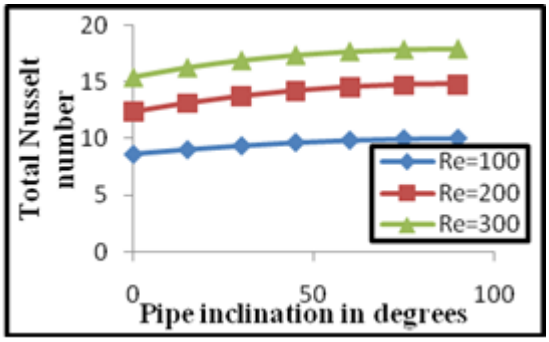

Fig. 5. Plot of total Nusselt number with inclination for F=4, R.R=0.1, Pr=0.73, W=0.2, β=3°

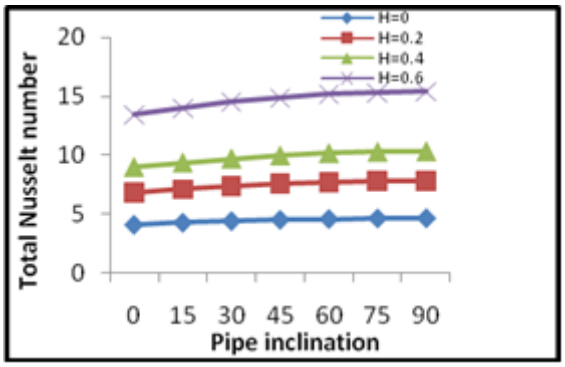

Fig. 6. Variation of total Nusselt number with inclination for :F=4,R.R=0.1,W=0.2, β=3°

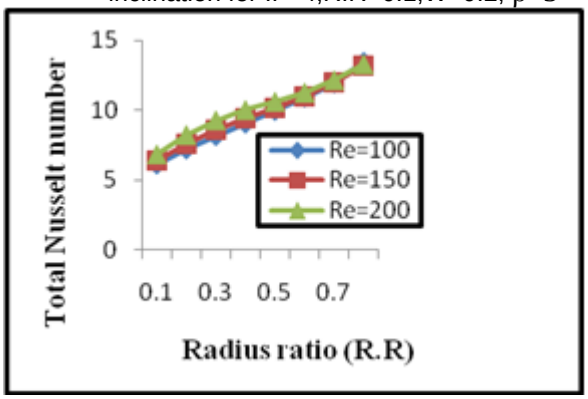

Fig. 7. Total Nusselt number versus radius ratio FOR: Pr=0.73, H=0.2, F=4, W=0.2, Ω =0° β=3°

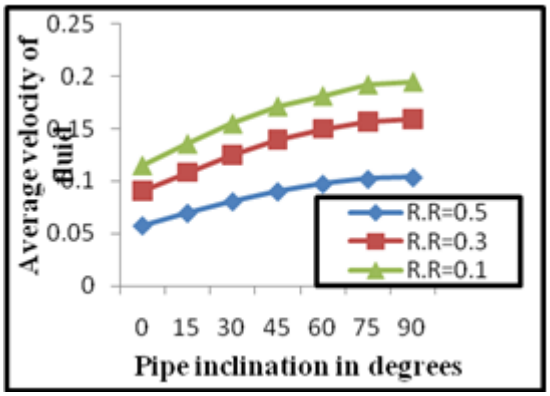

Fig. 8. Variation of average velocity with pipe inclination for different radius ratios for Pr=0.73, F=4, β=3°, W=0.2

range $0^{\circ} \leq \Omega \leq 75^{\circ}$ but for $75^{\circ} \leq \Omega \leq 90^{\circ}$, the average velocity becomes almost invariant with pipe inclination for all the plots. In this range of inclination, the effect of gravity on the flow becomes insignificant. Also it can be noticed that as the radius ratio increases the velocity of the fluid decreases this is as a result of increased fluid friction due to increase in the surface area of the pipe in contact with the fluid. As the wetted area increases due to increase in inner radius, the annulus cross sectional area reduces and therefore serve as constriction to the flow.

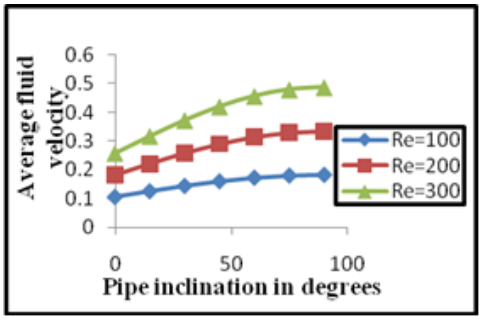

Fig. 9. Variation of average fluid velocity with inclination for : F=4, R.R=0.2, Pr=0.73 W=0.2, H=0.2, β=3°

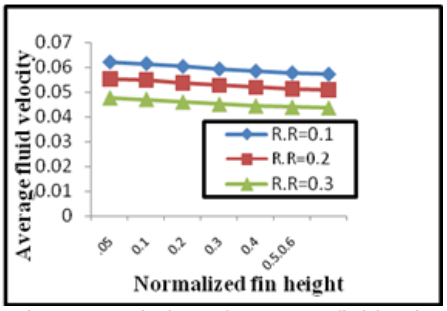

Fig. 10. Variation of average fluid velocity FOR:F=4,W=0.2, Pr=0.73, Ω =0°, β=3°

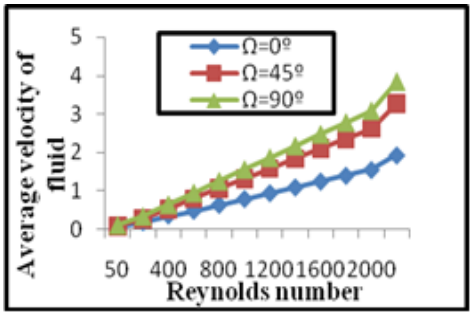

Fig. 11. Variation of average velocity of fluid with Reynolds number for: Pr=0.73, W=0.2, R.R=0.2, F=0.4

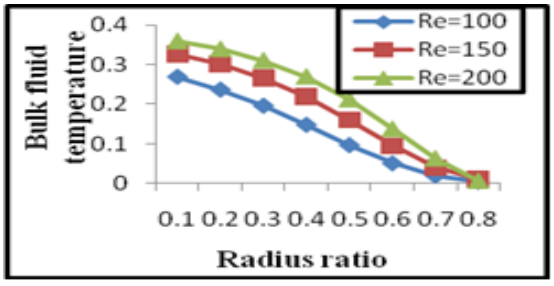

Fig. 12. Bulk fluid temperature versus R.R for varying Reynolds number for: Pr=0.73,W=0.2, H=0.2, Ω =0°

Figure 9 presents the variation of average fluid velocity with pipe inclination for various Reynolds numbers. The plots show a similar trend to that of Figure 8. Furthermore observation of the figure shows that velocity increases for all Reynolds numbers.

Figure 10 presents the variation of average velocity with fin height for varying radius ratios. The average velocity of fluid reduces with increase in the height of protrusion. This reduction may be connected to obstruction caused by the fins to the fluid flow. It can also be observed from the plots that the average velocity of the fluid decreases with increase in the radius ratio; this trend is supported by Figure 8.

Figure 11 depicts the plots of average fluid velocity as a function of Reynolds number for varying inclinations. The plots show that average velocity of fluid increases with

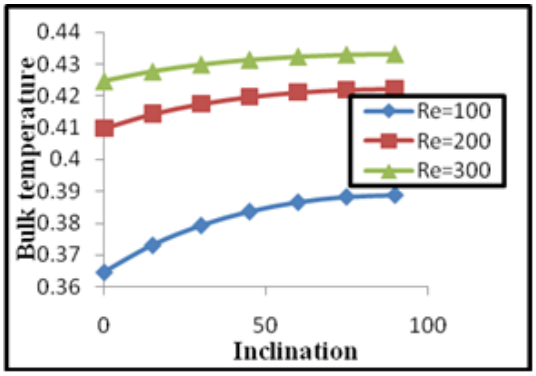

Fig. 13. Variation of total Nusselt number with inclination for: F=4, H=0.2, R.R=0.2 W = 0.2, Pr = 0.73, β=3°

both Reynolds number and inclination angles. These trends show that the more the pumping power of the machine the more the velocity of fluid for a given inclination.

Figure 12 shows the variation of bulk temperature with radius ratio for different Reynolds numbers. The plots show that bulk temperature of the fluid reduces with increase in radius ratio but increases with increase in Reynolds number. It can be concluded that high pumping power results in high bulk fluid temperature.

Figure 13 depicts the variation of bulk fluid temperature with pipe inclination over some selected Reynolds numbers. In the range $0^{\circ} \leq \Omega \leq 75^{\circ}$, the bulk fluid temperature increases with increase in pipe orientation but in the range $75^{\circ} \leq \Omega \leq 90^{\circ}$, the bulk fluid temperature does not show a significant increase with increase in pipe

inclination. This shows that in the range $75° \leq \Omega \leq 90°$ gravity has no significant effect on bulk fluid temperature.

Figure 14 presents the variation of bulk fluid temperature with Reynolds number for varying Prandtl numbers. For $50 \leq Re \leq 600$, the bulk fluid temperature increases with Reynolds number for fluids of different properties. For $Re > 600$, for the three fluids, the bulk fluid temperature does not increase significantly with increase in Reynolds number. Hence the geometry under investigation is better operated at a low Reynolds number flow regime because more cost would be required for higher pumping power.

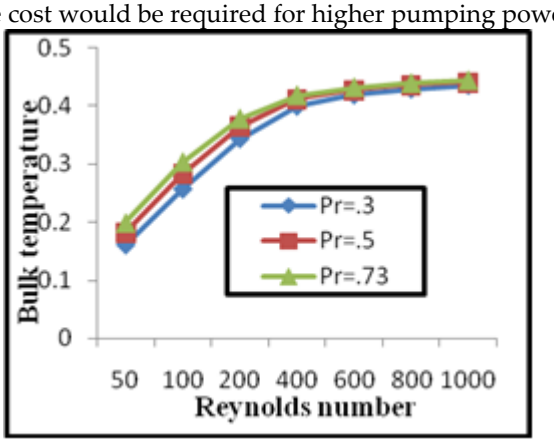

Fig. 14. Variation Of Bulk Temperature with Reynolds Number For: F=4, H=0.2,R.R=0.2, W=0.2,Pr=0.73, β=3°

Figure 15 shows the plots of bulk fluid temperature against pipe inclination for different radius ratios. The figure shows that the bulk fluid temperature decreases with increase in radius ratio-this shows that as the wetted surface area of the configuration under study increases the bulk temperature of the fluid decreases. Figure 15 shows the same trend as Figure 13, Furthermore, bulk fluid temperature reduces with increase in radius ratio, this is supported by Figure 12.

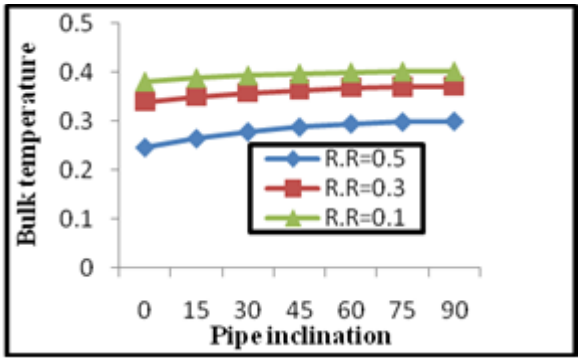

Fig. 15. Variation of fluid bulk temperature with pipe inclination for different radius ratios for: Pr=0.73, b=3°, H=0.2, W=0.2

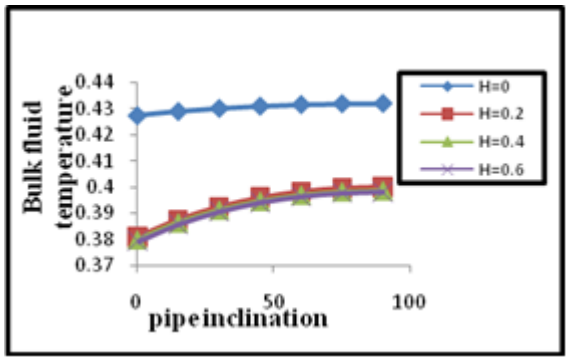

Fig. 16. Variation of bulk fluid temperature with pipe inclination for: F=4, b=3° R.R=0.1, Pr=0.73, W=0.2

Figure 16 is the variation of the bulk fluid temperature with pipe inclination for different fin heights. The plots show the same trend as figures 13 and 15. In the interval $0° \leq \Omega \leq 75°$, the bulk fluid temperature increases as pipe inclination increase but in the range $75° \leq \Omega \leq 90°$, the bulk fluid temperature does not show much increase with increase in pipe inclination. Furthermore as the fin height increases the bulk temperature of the fluid decreases showing that increase in the height of protrusion introduced into the walls of the protrusion results in decrease in bulk fluid temperature.

5 Conclusion

Having completed a detailed numerical study of the geometry investigated, the conclusions are made:

- For a fluid flow of Reynolds number, Re > 500, optimum bulk fluid temperature which is independent of fluid properties is achievable; also, for this range of flow, there is no significant increase in total Nusselt number.
- For this configuration, Nusselt number, the average velocity of fluid and bulk fluid temperature increase significantly with increase in pipe inclination in the range $0° \leq \Omega \leq 75°$ while there is no significant increase in each of these values in the range of $75° \leq \Omega \leq 90°$ .Hence, for reasonable heat transfer enhancement, the inclination of the pipe should not be greater than $75°$.
- For radius ratio R.R > 0.6, the heat transfer is almost independent of Reynolds number.
- For optimal use the configuration, the following parameter combination is recommended: Re=500, R.R. =0.6, H=0.6 , $\Omega = 75^0$

References

Adegun, I.K., & Bello-Ochende, F.L. (2004), *Laminar Mixed Convective and Radiative Heat Transfer in an Inclined Rotating Rectangular Duct with a Centered Circular Tube, Journal of the Brazilian Society of Mechanical Sciences- RBCM*, Vol. 26, No. 3, pp. 323-329.

Adegun, I.K. (2007), *Analytical Study of Fluid Flow and Heat Transfer in the Entrance Region of Heated Concentric Elliptic Annuli,* Unilorin Science and Engineering Periodicals, Journal of Research Information in Civil Engineering, Vol. 4, No. 1, pp. 68-85.

Chauhan, A.K., Prasad, B., & Patnaik, B. (2014), *Numerical simulation of flow through an eccentric annulus with heat transfer*, International Journal of Numerical Methods for Heat and Fluid Flow, Vol. 24, pp. 1864-1887.

Das, S. K. (2005), *Process Heat Transfer,* New York: Alpha Science Int'l Ltd.

Dirker, J., & Meyer, J. P. (2002), *Heat Transfer Coefficients In Concentric Annuli*, Journal of Heat Transfer, Vol. 124, pp.1200-1203.

Dogan, M., & Sivrioglu, M. (2010), *Experimental Investigation Of Mixed Convection Heat Transfer From Longitudinal Fins In A Horizontal Rectangular Channel*, International Journal of Heat and Mass Transfer, Vol. 53, pp. 2149-2158.

Dou, H.-S., Khoo, B. C., & Tsai, H. M. (2010), *Determining the Critical Condition for Flow Transition in a Full-Developed Annulus Flow*, Journal of Petroleum Science and Engineering, Vol. 71, pp. 1-20.

Ebrahim, N. H., El-Khatib, N., & Awang, M. (2013), *Numerical Solution of Power-Law Fluid Flow through Eccentric Annular Geometry,* American Journal of Numerical Analysis, Vol.1, pp. 1-7.

Haramoto, Y., Singai, M., & Ohba, H. (2002), *"The Flow around an Inclined Circular Cylinder and Aerodynamics Sound.* JSME Annual Meeting, Vol.6, pp. 121-122.

Incropera, F. P., & Dewitt, D. P. (2002), *Fundamentals of Mass and Heat Transfer,* Australia: John Willey and Sons.

Ishima, *T., Sasaki T., Gokan, Y., Takahshi, Y., Obokata, T.* (2008), *Flow Characteristics around an Inclined Circular Cylinder with Fin*. Proceedings of 14th Int Symp on Applications of Laser Techniques to Fluid Mechanics,(2008-7), pp. 1-10.

Jawarneh, A. (2007), *Heat Transfer Enhancement in Swirl Annulus Flows. Momentum,* Vol. 10, pp. 1.

Kakaç, S., & Yücel, O. (1974), *Laminar Flow Heat Transfer in an Annulus with Simultaneous Development of Velocity and Temperature Fields,* Technical and Scientific Concil of Turkey, TURBITAK, ISITEK, Ankara, Turkey, No.19.

Kang, M.G. (2008), *Effects of The Inclination Angle on Pool Boiling in an Annulus,* International Journal of Heat and Mass Transfer, Vol. 51, pp. 5018-5023.

Khalil, *M.F., Kassab, S.Z., Adam, I.G., Samaha, M.* (2008), *Laminar Flow in Concentric Annulus with a Moving Core,* 12th International Water Technology Conference Proceedings, IWTC12, pp.439-457.

Mir, N., Syed, K., & Iqbal, M. (2004), *Numerical Solution of Fluid Flow and Heat Transfer in the Finned Double Pipe,* Journal of Research (Science), Vol. 15. pp. 253-262.

Nobari, M., & Mehrabani, M. (2010), *A Numerical Study of Fluid Flow and Heat Transfer in Eccentric Curved Annuli,* International Journal of Thermal Sciences, Vol. 49, pp. 380-396.

Padilla,E.L.M., & Silveira-Neto R. C. A. (2006), *Numerical Analysis of the Natural Convection in Horizontal Annuli at Low and Moderate Rayleigh Number,* Engenharia Termica(Thermal Engineering), Vol. 5, pp. 58-65.

Rafee, R. (2014*), Entropy Generation Calculation For Laminar Fully Developed Forced Flow and Heat Transfer of Nanofluids Inside Annuli.* Journal of Heat and Mass Transfer Research (JHMTR), Vol. 1, pp. 25-33.

Welty, J. R. (1974), *Engineering Heat Transfer*, New York: John Wiley and Sons, Inc.

Wu, F., & Zhou, W. (2015), *Numerical Simulation of Convective Heat Transfer and Pressure Drop in Two Types of Longitudinally and Internally Finned Tubes*, Vol. 46, pp. 31-48.

NOMENCLATURE

Cp	Fluid specific heat, kJ/kgk	Re_m	Modified Reynolds number
F	Number of fins	T	Dimensional Temperature, ^{0}C
G	Acceleration due to gravity, m/s^2	T_f	Dimensional Temperature of fluid, ^{0}C
g_x	Acceleration due to gravity in the axial direction, m/s^2	T_o	Uniform entry temperature, ^{0}C
H	Fin height, m	T_w	Wall temperature , ^{0}C
H	Dimensionless fin height	U	Dimensionless velocity
K	Iteration counter	V_x	Velocity in the axial direction, m/s
k_f	Thermal conductivity of fluid, W/mk	V_r	Velocity in the radial direction, m/s
k_s	Thermal conductivity of wall, W/mk	V_Θ	Velocity in the azimuthal direction. m/s
k^*	Ratio of thermal conductivity of wall to thermal conductivity of fluid	w	Wall thickness, m
Nu_i	Inner wall Nusselt	W	Dimensionless wall
Nu_o	number	∂	thickness
P	Outer wall Nusselt		Partial differential
Pe	number	α	**Greek Symbol**
Pe'	Pressure , N/m^2	α_t	Angle between fin tips, in degrees
	Peclet number(Re.Pr)		Thermal diffusivity, m^2/s
	Modified Peclet number(P_kPe)		
P_k	Parameter for modification of Peclet number	β	Fin half angle
Pr	Prandtl number	Γ	Normalized axial distance
q_o	Heat flux in the inner wall of the outer Pipe, W/m^2	δ	Maximum error
q_{Ro+w}	Heat flux in the outer wall of the outer pipe, W/m^2	ε	Limit
r	Variable pipe radius, m	θ	Azimuthal direction
R	Dimensionless radius of pipe	λ	Analytical solution of the differential equation
Re	Reynolds number	λ^*	Numerical solution of the governing equation
R.R	Radius ratio	μ	Dynamic viscosity, N.s/m^2
R_{in}	Dimensional inner radius of pipe, m	ϕ	Dimensionless temperature
R_o	Dimensional outer radius of pipe, m	Ω	Pipe inclination angle, in degrees